Check for updates

Biopolymers

Special Issue: Peptoids – Part 1

Guest Editors: Kent Kirshenbaum (New York University, U.S.A.) and Ronald N. Zuckermann (Lawrence Berkeley National Laboratory, U.S.A.)

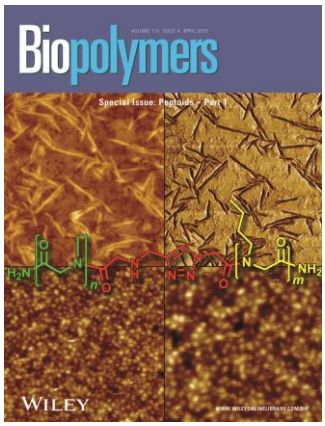

EDITORIAL

Peptoids in Wonderland
Kent Kirshenbaum and Ronald N. Zuckermann, *Biopolymers* 2019, doi: 10.1002/bip.23279

REVIEW

Design and preparation of organic nanomaterials using self-assembled peptoids
Alessia Battigelli, *Biopolymers* 2019, doi: 10.1002/bip.23265

FULL PAPERS

Dual-responsive pegylated polypeptoids with tunable cloud point temperatures
Xiaohui Fu, Jiliang Tian, Zheng Li, Jing Sun and Zhibo Li, *Biopolymers* 2019, doi: 10.1002/bip.23243

Solid-phase synthesis of three-armed star-shaped peptoids and their hierarchical self-assembly
Haibao Jin, Tengyue Jian, Yan-Huai Ding, Yulin Chen, Peng Mu, Lei Wang and Chun-Long Chen, *Biopolymers* 2019, doi: 10.1002/bip.23258

Polymerization rate difference of *N*-alkyl glycine NCAs: Steric hindrance or not?
Tianwen Bai and Jun Ling, *Biopolymers* 2019, doi: 10.1002/bip.23261

Linking two worlds in polymer chemistry: The influence of block uniformity and dispersity in amphiphilic block copolypeptoids on their self-assembly
Niklas Gangloff, Marcel Höferth, Vladimir Stepanenko, Benedikt Sochor, Bernhard Schummer, Joachim Nickel, Heike Walles, Randolf Hanke, Frank Würthner, Ronald N. Zuckermann and Robert Luxenhofer, *Biopolymers* 2019, doi: 10.1002/bip.23259

Peptoids advance multidisciplinary research and undergraduate education in parallel: Sequence effects on conformation and lipid interactions
Christian J. Jimenez, Jiacheng Tan, Kalli M. Dowell, Gillian E. Gadbois, Cameron A. Read, Nicole Burgess, Jesus E. Cervantes, Shannon Chan, Anmol Jandaur, Tara Karanik, Jaenic J. Lee, Mikaela C. Ley, Molly McGeehan, Ann McMonigal, Kira L. Palazzo, Samantha A. Parker, Andre Payman, Maritza Soria, Lauren Verheyden, Vivian T. Vo, Jennifer Yin, Anna L. Calkins, Amelia A. Fuller and Grace Y. Stokes, *Biopolymers* 2019, doi: 10.1002/bip.23256

Phosphoramitoids—A submonomer approach to sequence defined *N*-substituted phosphoramidate polymers
Thomas Horn, Michael D. Connolly and Ronald N. Zuckermann, *Biopolymers* 2019, doi: 10.1002/bip.23268

Solution effects on the self-association of a water-soluble peptoid
Amelia A. Fuller, Jonathan Huber, Christian J. Jimenez, Kalli M. Dowell, Samuel Hough, Alberto Ortega, Kyra N. McComas, Jeffrey Kunkel and Prashanth Asuri, *Biopolymers* 2019, doi: 10.1002/bip.23248

Biopolymers

Special Issue: Peptoids – Part 1

Guest Editors: Kent Kirshenbaum (New York University, U.S.A.) and Ronald N. Zuckermann (Lawrence Berkeley National Laboratory, U.S.A.)

A facile on-bead method for fully symmetric tetra-substituted DOTA derivatizations using peptoid moieties
Vineeta Rustagi and D. Gomika Udugamasooriya, *Biopolymers* 2019, doi: 10.1002/bip.23249

Macrocyclization enhances affinity of chemokine-binding peptoids
Kevin Brahm, Julia S. Wack, Stefanie Eckes, Victoria Engemann and Katja Schmitz, *Biopolymers* 2019, doi: 10.1002/bip.23244

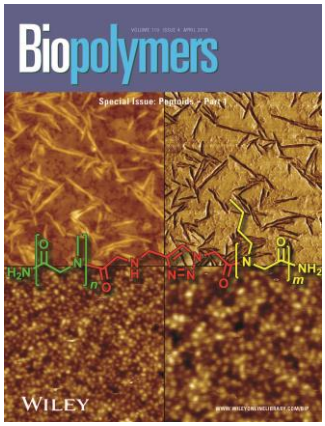

10970282, 2019, 6, Downloaded from https://onlinelibrary.wiley.com/doi/10.1002/bip.23267 by University Of California, Wiley Online Library on [10/02/2026]. See the Terms and Conditions (https://onlinelibrary.wiley.com/terms-and-conditions) on Wiley Online Library for rules of use; OA articles are governed by the applicable Creative Commons License

Biopolymers

Special Issue: Peptoids – Part 2

Guest Editors: Kent Kirshenbaum (New York University, U.S.A.) and Ronald N. Zuckermann (Lawrence Berkeley National Laboratory, U.S.A.)

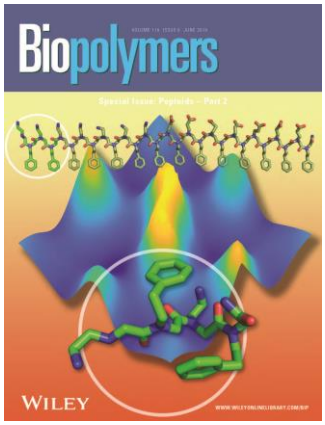

EDITORIAL

Molecular folding science
Kent Kirshenbaum and Ronald N. Zuckermann, *Biopolymers* 2019, doi: 10.1002/bip.23314

REVIEWS

Peptoids as tools and sensors
Adrian S. Culf, *Biopolymers* 2019, doi: 10.1002/bip.23285

Peptoid drug discovery and optimization via surface X-ray scattering
Konstantin Andreev, Michael W. Martynowycz and David Gidalevitz, *Biopolymers* 2019, doi: 10.1002/bip.23274

Polypeptoids synthesis based on Ugi reaction: Advances and perspectives
Yue Tao, Zhen Wang and Youhua Tao, *Biopolymers* 2019, doi: 10.1002/bip.23288

FULL PAPERS

NCα-gem-dimethylated peptoid side chains: A novel approach for structural control and peptide sequence mimetics
Radhe Shyam, Lionel Nauton, Gaetano Angelici, Olivier Roy, Claude Taillefumier and Sophie Faure, *Biopolymers* 2019, doi: 10.1002/bip.23273

Unconstrained peptoid tetramer exhibits a predominant conformation in aqueous solution
Leah T. Roe, Jeffrey G. Pelton, John R. Edison, Glenn L. Butterfoss, Blakely W. Tresca, Bridgette A. LaFaye, Stephen Whitelam, David E. Wemmer and Ronald N. Zuckermann, *Biopolymers* 2019, doi: 10.1002/bip.23267

Oligomers of α-ABpeptoid/β^3-peptide hybrid
Kang Ju Lee, Ganesh A. Sable, Min-Kyung Shin and Hyun-Suk Lim, *Biopolymers* 2019, doi: 10.1002/bip.23289

Stereochemistry of polypeptoid chain configurations
Ryan K. Spencer, Glenn L. Butterfoss, John R. Edison, James R. Eastwood, Stephen Whitelam, Kent Kirshenbaum and Ronald N. Zuckermann, *Biopolymers* 2019, doi: 10.1002/bip.23266

Peptoid microsphere coatings: The effects of helicity, temperature, pH, and ionic strength
German R. Perez Bakovic, Jesse L. Roberts, Bryce Colford, Myles Joyce and Shannon L. Servoss, *Biopolymers* 2019, doi: 10.1002/bip.23283

Antibacterial mechanisms of GN-2 derived peptides and peptoids against *Escherichia coli*
Paola Saporito, Mojsoska Biljana, Anders Løbner Olesen and Håvard Jenssen, *Biopolymers* 2019, doi: 10.1002/bip.23275

Toward a clinical antifungal peptoid: Investigations into the therapeutic potential of AEC5
Sabrina K. Spicer, Aarthi Subramani, Angelica L. Aguila, R. Madison Green, Erin E. McClelland and Kevin L. Bicker, *Biopolymers* 2019, doi: 10.1002/bip.23276

Helical side chain chemistry of a peptoid-based SP-C analogue: Balancing structural rigidity and biomimicry
Nathan J. Brown, Jennifer S. Lin and Annelise E. Barron, *Biopolymers* 2019, doi: 10.1002/bip.23277

10970282, 2019, 6, Downloaded from https://onlinelibrary.wiley.com/doi/10.1002/bip.23267 by University Of California, Wiley Online Library on [10/02/2026]. See the Terms and Conditions (https://onlinelibrary.wiley.com/terms-and-conditions) on Wiley Online Library for rules of use; OA articles are governed by the applicable Creative Commons License

Received: 18 November 2018 | Revised: 29 January 2019 | Accepted: 12 February 2019
DOI: 10.1002/bip.23267

Biopolymers WILEY

FULL PAPER

Unconstrained peptoid tetramer exhibits a predominant conformation in aqueous solution

Leah T. Roe[1] | Jeffrey G. Pelton[2] | John R. Edison[1] | Glenn L. Butterfoss[3] | Blakely W. Tresca[1,4] | Bridgette A. LaFaye[1] | Stephen Whitelam[1] | David E. Wemmer[5] | Ronald N. Zuckermann[1]

[1]The Molecular Foundry, Lawrence Berkeley National Laboratory, Berkeley, California
[2]QB3 Institute, University of California, Berkeley, California
[3]Center for Genomics and Systems Biology, New York University Abu Dhabi, Abu Dhabi, United Arab Emirates
[4]Department of Chemistry, Kalamazoo College, Kalamazoo, Michigan
[5]Department of Chemistry, University of California, Berkeley, California

Correspondence
Ronald N. Zuckermann, The Molecular Foundry, Lawrence Berkeley National Laboratory, 1 Cyclotron Rd., Berkeley, CA 94720.
Email: rnzuckermann@lbl.gov

Funding information
Basic Energy Sciences, Grant/Award Number: DE-AC02-05CH11231; Defense Advanced Research Projects Agency, Grant/Award Number: Fold F(x) program; National Institutes of Health, Grant/Award Number: GM68933

Abstract

Conformational control in peptoids, *N*-substituted glycines, is crucial for the design and synthesis of biologically-active compounds and atomically-defined nanomaterials. While there are a growing number of structural studies in solution, most have been performed with conformationally-constrained short sequences (e.g., sterically-hindered sidechains or macrocyclization). Thus, the inherent degree of heterogeneity of unconstrained peptoids in solution remains largely unstudied. Here, we explored the folding landscape of a series of simple peptoid tetramers in aqueous solution by NMR spectroscopy. By incorporating specific ^{13}C-probes into the backbone using bromoacetic acid-2-^{13}C as a submonomer, we developed a new technique for sequential backbone assignment of peptoids based on the 1,*n*-Adequate pulse sequence. Unexpectedly, two of the tetramers, containing an *N*-(2-aminoethyl)glycine residue (Nae), had preferred conformations. NMR and molecular dynamics studies on one of the tetramers showed that the preferred conformer (52%) had a *trans-cis-trans* configuration about the three amide bonds. Moreover, >80% of the ensemble contained a *cis* amide bond at the central amide. The backbone dihedral angles observed fall directly within the expected minima in the peptoid Ramachandran plot. Analysis of this compound against similar peptoid analogs suggests that the commonly used Nae monomer plays a key role in the stabilization of peptoid structure via a side-chain-to-main-chain interaction. This discovery may offer a simple, synthetically high-yielding approach to control peptoid structure, and suggests that peptoids have strong intrinsic conformational preferences in solution. These findings should facilitate the predictive design of folded peptoid structures, and accelerate application in areas ranging from drug discovery to biomimetic nanoscience.

KEYWORDS

peptoid structure, 2D NMR, conformational control, molecular dynamics

1 | INTRODUCTION

The peptoid backbone without any imposed conformational constraint is considered to be flexible.[1,2] To design effective drugs or protein mimetic materials from peptoids, it is essential to understand and control their conformation. Thus, researchers have developed a variety of methods to constrain peptoid structure, including macrocyclization,[3] steric congestion,[4,5] side chain chirality,[5–7] and electronic interactions.[8,9] Most of these rely on bulky, hydrophobic groups, which can dominate the molecular properties and restrict water solubility, hindering the development of biological applications. As a result, most peptoid structures obtained thus far have been determined in either the solid state or in organic solvent.[10]

To better understand the solution structure of minimally constrained peptoids in water, we examine a family of tetramers that contain simple ethyl-substituted side chains that have been widely used in peptoid science: *N*-(2-phenylethyl)glycine (Npe), *N*-(2-aminoethyl)glycine (Nae), and *N*-(2-carboxyethyl)glycine (Nce). These three monomers, when arranged

 © 2019 Wiley Periodicals, Inc.

10970282, 2019, 6, Downloaded from https://onlinelibrary.wiley.com/doi/10.1002/bip.23267 by University Of California, Wiley Online Library on [10/02/2026]. See the Terms and Conditions (https://onlinelibrary.wiley.com/terms-and-conditions) on Wiley Online Library for rules of use; OA articles are governed by the applicable Creative Commons License

in longer chains with an alternating aromatic-ionic sequence motif, form highly ordered supramolecular nanosheets in aqueous solution. Peptoid nanosheets are a functionally diverse class of materials[11] that show great promise as affinity reagents, templates for mineralization, and as cell-surface mimetics. Nanosheets have a well-defined molecular structure with their backbones containing primarily *cis* amide bonds,[12] as determined by solid-state NMR, X-ray diffraction, electron microscopy and atomic force microscopy, despite being comprised of only these three sterically unhindered monomers. However, because the nanosheets are micron-scale objects (in length and width) and tumble very slowly in solution, their detailed molecular conformations cannot be probed by solution NMR, which is very often the technique of choice for studying molecular structure and dynamics in solution.

NMR is often used to determine the solution structure of moderately-sized proteins.[13] The procedure typically involves uniform ^{15}N and ^{13}C isotope labeling via bacterial expression using ^{15}N ammonium chloride and ^{13}C glucose as the sole nitrogen and carbon sources. For proteins predominately in a folded state, the well-dispersed amide proton and nitrogen resonances provide a good starting point for resonance assignment and structure determination. Peptoid NMR structure determination, in contrast, involves several additional challenges. Because the peptoid backbone lacks an amide proton, assignments must center on the backbone CH_2 groups (the alpha carbons). The proton and carbon shifts of these methylene groups show poor dispersion relative to protein amide proton and nitrogen shifts, leading to spectral crowding. Crowding is further exacerbated by the fact that the amide bonds in peptoids tend to readily adopt both *cis* and *trans* conformations, leading to as many as $2^{(n-1)}$ amide states, for a peptoid of n residues. Fortunately, specific ^{13}C labeling at backbone CH_2 and carbonyl positions[14] is straightforward for peptoids, but labeling the sidechains is laborious, generally necessitating less sensitive natural abundance ^{13}C experiments. The problem with longer oligomers then becomes assigning and obtaining structural information on a growing number of resonances. The longest peptoid structure determined by solution NMR was a 9mer homo-oligomer of the hindered, structure-inducing monomer *N*-(1-phenylethyl)glycine.[7]

Herein, we present detailed solution NMR characterization of four peptoid tetramers. Tetramers were chosen to be short enough to characterize, but long enough to avoid chain termini effects. Unexpectedly, we found that two of the peptoids examined have preferred conformations in solution. The central residues in both these sequences are Npe-Nae, and we observe a clear preference for the amide bond between these two residues to be in the *cis* conformation.

2 | MATERIALS AND METHODS

2.1 | Peptoid synthesis

All peptoid tetramers were synthesized using the solid-phase submonomer method[15] at 50°C. Before starting the submonomer cycle, rink amide resin was first swelled in NMP for 10 minutes and then deprotected with 20% 4-methyl-piperidine in NMP for 10 minutes. During the bromoacetylation step of the submonomer cycle, the resin was treated with a 1:1 mixture of 2 M bromoacetic acid and 2 M *N*,*N*′-diisoproplycarbodiimide in NMP and mixed for 5 minutes. At steps where ^{13}C labeling was desired, bromoacetic acid-2-^{13}C was used in place of bromoacetic acid. The displacement step was carried out using a 1 M solution of the amine in NMP for a duration of 5 minutes. Crude peptoid products were cleaved from resin using a cocktail of 95:2.5:2.5 trifluorocetic acid (TFA):triisopropylsilane:water for 1 hour at room temperature. The cleavage solution was then filtered and the volatiles removed in vacuo using a Biotage V10 Evaporator. Crude peptoid product was dissolved into a 5:95 acetonitrile:water solution and further purified using reverse-phase chromatography on a Waters Prep150LC system with Waters 2489 UV/Visible Detector on a Waters XBridge BEH300 Prep C18 column using a 5-40% acetonitrile in water with 0.1% TFA gradient over 30 minutes. Final products were dissolved in water and lyophilized. All final products were analyzed by Waters Acquity UPLC system with Acquity Diode Array UV detector and Waters SQD2 mass spectrometer on a Waters Acquity UPLC Peptide BEH C18 Column over a 5-50% gradient.

2.2 | NMR spectroscopy

All NMR samples were prepared at a peptoid concentration of 10 mM solution in 90% D_2O and 10% 40 mM sodium phosphate buffer in water at pH 7.4. All peptoids are in the presence of TFA salt, and amino groups on Nae sidechains are expected to be protonated at pH 7.4.

NMR spectra (^1H and HSQC) for peptoids **1**-**4** were recorded on a Bruker Avance500 II, using locking to the deuterated solvent and using tetramethylsilane as an internal standard. All chemical shifts are quoted using the δ scale, and all coupling constants (J) are expressed in Hertz (Hz). Further NMR experiments for peptoids **1** and **5**-**9** were recorded on a Bruker-Biospin Inc Avance II NMR spectrometer operating at 900 MHz, and controlled with Topspin software (version 3.2) and equipped with a TCI cryoprobe at 25 °C.

2.2.1 | Peptoid 1

An edited ^1H-^{13}C HSQC spectrum of peptoid **1** was recorded using pulse sequence hsqcedetgpsisp2.2 using spectral widths of 16 ppm (^1H) and 165 ppm (^{13}C), carrier frequencies of 4.69 ppm (^1H) and 70 ppm (^{13}C), and with 1024 (^1H) and 128 complex points (^{13}C). A total of four scans were recorded for each t1 increment along with a recycle time of 2 seconds, resulting in an experiment time of 36 minutes.

A 2D ^1H-^{13}C HMBC experiment on peptoid **1** was recorded using pulse sequence hmbcgplpndqf using spectral widths of 11 ppm (^1H) and 222 ppm (^{13}C), carrier frequencies of 4.69 (^1H) and 100 ppm (^{13}C) and with 1024 (^1H) and 128 (^{13}C) complex points. The $^1J_{CH}$ and long-range J_{CH} coupling values were set to 145 Hz and 10 Hz, respectively. A total of 16 scans were recorded for each t1 increment with a recycle delay of 1.5 seconds, resulting in an experiment time of 57 minutes.

A gradient COSY experiment was recorded with pulse sequence cosygpqf using spectral widths of 16 ppm in both dimensions, carrier frequency of 4.69 ppm, and 2048 (direct dimension) and 128 complex points (indirect dimension). A total of four scans were averaged for each t1 increment and the recycle delay was set to 1.5 seconds, resulting in a total experiment time of 28 minutes.

A 2D ROESY experiment was recorded using pulse sequence roesyetgp.2 that was modified to include presaturation of the residual HDO

10970282, 2019, 6, Downloaded from https://onlinelibrary.wiley.com/doi/10.1002/bip.23267 by University Of California, Wiley Online Library on [10/02/2026]. See the Terms and Conditions (https://onlinelibrary.wiley.com/terms-and-conditions) on Wiley Online Library for rules of use; OA articles are governed by the applicable Creative Commons License

resonance during the recycle delay. The mixing time was composed of 100 μs 180_x,180_{-x} pulses applied for a total time of 300 ms. The spectrum was recorded with spectral widths of 11 ppm in each dimension, a carrier frequency of 4.69 ppm, and with 2048 complex points in the direct dimension, and 256 complex points in the indirect dimension. A total of 32 scans was used for each t1 increment, along with a recycle time of 2 seconds, resulting in an experiment time of 3 hours.

2.2.2 | Peptoids with ^{13}C-enriched backbones

A 2D ^{1}H-^{13}C HSQC experiment focused on the backbone ^{13}C resonances was recorded with spectral widths of 11 ppm (^{1}H) and 20 ppm (^{13}C) and with carrier frequencies set to 4.69 ppm and 50 ppm. A total of 1024 (^{1}H) and 128 complex points (^{13}C) were recorded using four scans and a recycle delay of 2 seconds, for a total experiment time of 36 minutes. Similar spectra were recorded on the singly labeled peptoids **6**-**9**. Because these data were used to quantify the abundance of each conformer, the delay between scans was increased to 4.25 seconds, to ensure that the magnetization was fully recovered between scans. For these experiments the total experiment time was 77 minutes.

A 2D 1,*n*-Adequate spectrum was recorded with pulse sequence adeq1netgprdsp using spectral widths of 11 ppm (^{1}H) and 20 ppm (^{13}C), carrier frequencies of 4.69 ppm (^{1}H) and 50 ppm (^{13}C),and with 1024 (^{1}H) and 128 (^{13}C) complex points. The $^1J_{CH}$, $^1J_{CC}$, $^nJ_{CC}$, and $^{n'}J_{CC}$ coupling constants were set to standard values of 145 Hz, 45 Hz, 9.5 Hz, and 8 Hz, respectively. Optimization of these parameters for the small three-bond couplings between backbone ^{13}C spins of neighboring residues, may improve the sensitivity of the experiment. A total of 16 scans per t1 increment were recorded and the recycle delay was set to 2 seconds, resulting in a total experiment time of 5 hours.

A 2D ^{1}H-^{13}C HSQC-ROESY experiment was recorded using pulse sequence hsqcetgprosp.2 with spectral widths of 6 ppm (^{1}H) and 10 ppm (^{13}C), carrier frequencies of 4.70 ppm (^{1}H) and 50 ppm (^{13}C) and 1024 (^{1}H) and 100 (^{13}C) complex points. Similar to the ^{1}H-^{1}H ROESY, the mixing time was composed of 100 μs 180x,180-x pulses applied for a total time of 300 ms. A total of 128 scans was used for each t1 increment, along with a recycle time of 2 seconds, resulting in a total experiment time of 18 hours.

2.2.3 | 3D experiments

Three dimensional hCCH-TOCSY and two HcCH-TOCSY experiments with different mixing times were recorded on peptoids **6**-**9** labeled with ^{13}C at each backbone position on a Bruker Avance 800 MHz spectrometer equipped with a room-temperature TXI probe operating at 25 °C. These experiments were designed for the assignment of the sidechain ^{1}H and ^{13}C signals of proteins, taking advantage of strong single-bond ^{13}C-^{13}C spin couplings (~35 Hz) and were optimized for the large chemical shift dispersion of protein sidechain ^{13}C resonances (~70 ppm). The three-bond ^{13}C-^{13}C spin couplings are significantly smaller (estimated to be less than 2 Hz), and the dispersion of the signals is significantly less (4 ppm). To account for these differences, the pulse sequences were unmodified, but the rf field strength of the mixing time was reduced to 1.67 kHz, and the duration was increased to 260 ms for complete transfer among the four carbon (hCCH-TOCSY) or proton (HcCH-TOCSY) resonances, and to 97.5 ms for limited transfer to adjacent proton spins.

In each experiment a total of 1024 (F3,^{1}H) and 24 (F1,^{13}C) complex points were recorded with spectral widths of 11 ppm (^{1}H) and 10 ppm (^{13}C), and carrier frequencies of 4.69 and 50 ppm. A total of 16 scans were averaged for each fid, and the recycle delay was set to 2 seconds.

In the hCCH-TOCSY experiment (pulse sequence hcchdigp3d2), the mixing time was set to 260 ms, and 32 complex points were collected in the indirect TOCSY dimension (F2, ^{13}C). The experiment was recorded in 33.5 hours. In the HcCH-TOCSY experiment (pulse sequence hcchdigp3d), 128 complex points were collected in the indirect TOCSY dimension (F2, ^{1}H). The HcCH-TOCSY experiments with the longer, and shorter mixing times were recorded in 67 hours, and 62.5 hours, respectively.

2.3 | Molecular dynamics

NAMD simulation[16] package was used for our classical Molecular Dynamics simulations. The interactions between the peptoid residues were described by the MFTOID forcefield[17] developed at the Molecular Foundry. A single peptoid was solvated in a cubic water box of size (40 Å × 40 Å × 40 Å). Two negatively charged ions were added to the system to keep it net neutral. We used the TIP3P potential to describe the interactions of water molecules. The SHAKE algorithm was used to fix the positions of the hydrogen atoms. Short range interactions were cut-off at 12 Å and electrostatic interactions were estimated using Ewald summation with a grid spacing of 1 Å. The integration time step was set to 1 fs. A Langevin thermostat was used to fix the temperature at 298 K. The system was initially equilibrated in the NPT ensemble for 1 ns, followed by an NVT run for 10 ns. The simulation trajectory is provided as supporting information and consists of 10 structures taken at equal time intervals over the 10 ns simulation.

2.4 | Quantum mechanics

All DFT modeling was done with Gaussian16.[18] DFT analysis of peptoid **1** began with 30 starting conformations: 20 extracted from periodic snapshots of the unrestrained *trans-cis-trans* MD trajectory described above, and 10 were built manually (also with a *trans-cis-trans* amide pattern). The 30 structures were initially optimized with +2 charges and protonated Nae sidechains at the B3LYP/6-31G* level of theory (in vacuo) and the 12 lowest energy structures (0-14.3 kcal/mol range of relative energies) were selected. These 12 were further geometry optimized at both the B3LYP/6-311G** (with PCM) and M06-2X/6-311G** (with PCM) levels of theory.

3 | RESULTS AND DISCUSSION

3.1 | Structural survey of peptoid tetramers

We selected a set of four peptoid tetramers, three of which represent short sections of the nanosheet-forming sequence, Block28 (Figure 1).[12] Peptoids **1** and **2** were taken from the amino and carboxy termini, respectively, while peptoid **4** is taken from the center of the chain. Peptoid **3** is a control sequence. Tetramer segments were chosen for ease of

10970282, 2019, 6, Downloaded from https://onlinelibrary.wiley.com/doi/10.1002/bip.23267 by University Of California, Wiley Online Library on [10/02/2026]. See the Terms and Conditions (https://onlinelibrary.wiley.com/terms-and-conditions) on Wiley Online Library for rules of use; OA articles are governed by the applicable Creative Commons License

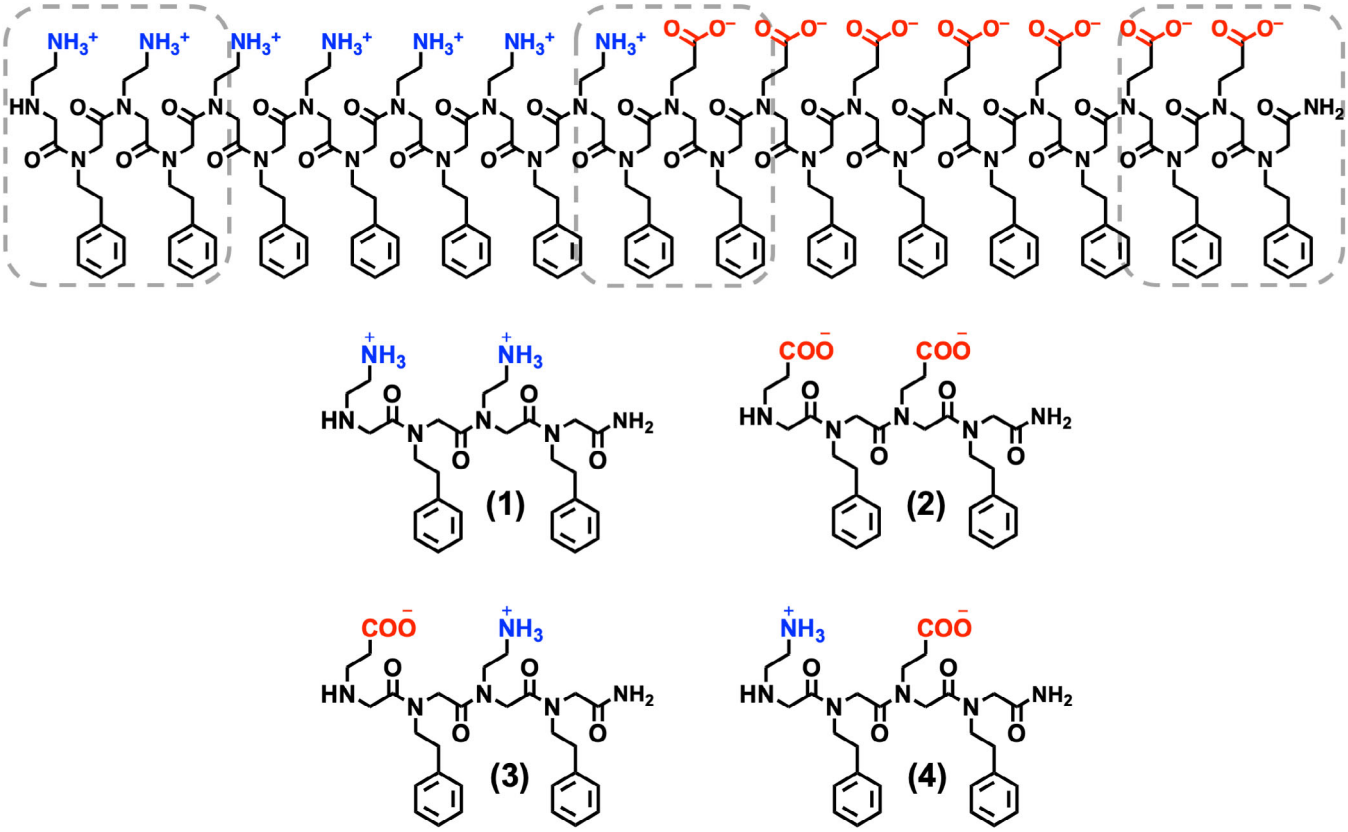

FIGURE 1 The nanosheet forming sequence, Block28 (above), was broken into a series of shorter tetramer sequences in order to examine their conformational preferences by solution NMR

structural analysis, and to mimic the interior of longer peptoid chains. Peptoids **1**-**4** were synthesized by the solid-phase submonomer method and purified to homogeneity by reverse-phase HPLC (Table 1). These four peptoids were dissolved in 90% D_2O and 10% sodium phosphate buffer at pH 7.4 in water and analyzed for structural homogeneity using NMR.

1D ^{1}H and 2D ^{1}H-^{13}C HSQC experiments were used to identify the presence or absence of a major conformation in solution for the four tetramers.[19] As can be seen in Figure 2, peptoids **1** (Figure 2A) and **3** (Figure 2C) exhibit preferred conformations (e.g., four distinct backbone methylene singlet peaks), while peptoids **2** (Figure 2B) and **4** (Figure 2D) show less conformational preference. The ^{1}H peaks for peptoid **2** were broader, indicating conformational exchange on the millisecond time scale. Notably, the most ordered peptoids, **1** and **3**, both have Npe-Nae in the central two positions, suggesting these residues have a role in driving a preferred conformation. Because compound **1** appeared to be the most conformationally-defined, it was chosen for detailed analysis of its major and minor conformations by 2D and 3D NMR.

3.2 | Peptoid 1 major conformation structural analysis

Peptoid **1** has 12 methylene groups—four in the backbone (BB) and eight in the side chains (SC)—that serve as the principal guideposts for determining the structure (see Figure 3 for naming convention). The general method for structure assignment follows: (a) HSQC to assign ^{1}H-^{13}C connections of the major conformation, (b) COSY to group SC methylenes by residue, (c) HMBC to connect SCs to BBs and assign monomer type, (d) 1,*n*-Adequate to place residues in sequence order, and (e) ROESY to identify key through space interactions between protons.

3.3 | HSQC

An HSQC experiment was used to verify the presence of a major conformation, and correlate the 12 methylene carbons to their attached hydrogens. For peptoid **1**, the presence of 12 intense distinct correlations indicated that one conformation predominates in solution (Figure 4). This is in contrast to peptoids **2** and **4**, where the HSQC spectra of both showed at least 24 correlations at a similar

TABLE 1 Peptoid tetramer sequences

Peptoid	Sequence	Expected mass	Observed mass	Purity[a]
1	Nae-Npe-Nae-Npe	540.3	540.5	>99%
2	Nce-Npe-Nce-Npe	597.3	598.0	>99%
3	Nce-Npe-Nae-Npe	568.3	569.0	>99%
4	Nae-Npe-Nce-Npe	568.3	570.0	>99%
5	Nae[b]-Npe[b]-Nae[b]-Npe[b]	544.3	544.5	>99%
6	Nae[b]-Npe-Nae-Npe	541.3	541.5	>99%
7	Nae-Npe[b]-Nae-Npe	541.3	542.0	>99%
8	Nae-Npe-Nae[b]-Npe	541.3	541.2	>99%
9	Nae-Npe-Nae-Npe[b]	541.3	542.0	>99%

[a]After HPLC purification.
[b]Contains ^{13}C at the alpha carbon.

10970282, 2019, 6, Downloaded from https://onlinelibrary.wiley.com/doi/10.1002/bip.23267 by University Of California, Wiley Online Library on [10/02/2026]. See the Terms and Conditions (https://onlinelibrary.wiley.com/terms-and-conditions) on Wiley Online Library for rules of use; OA articles are governed by the applicable Creative Commons License

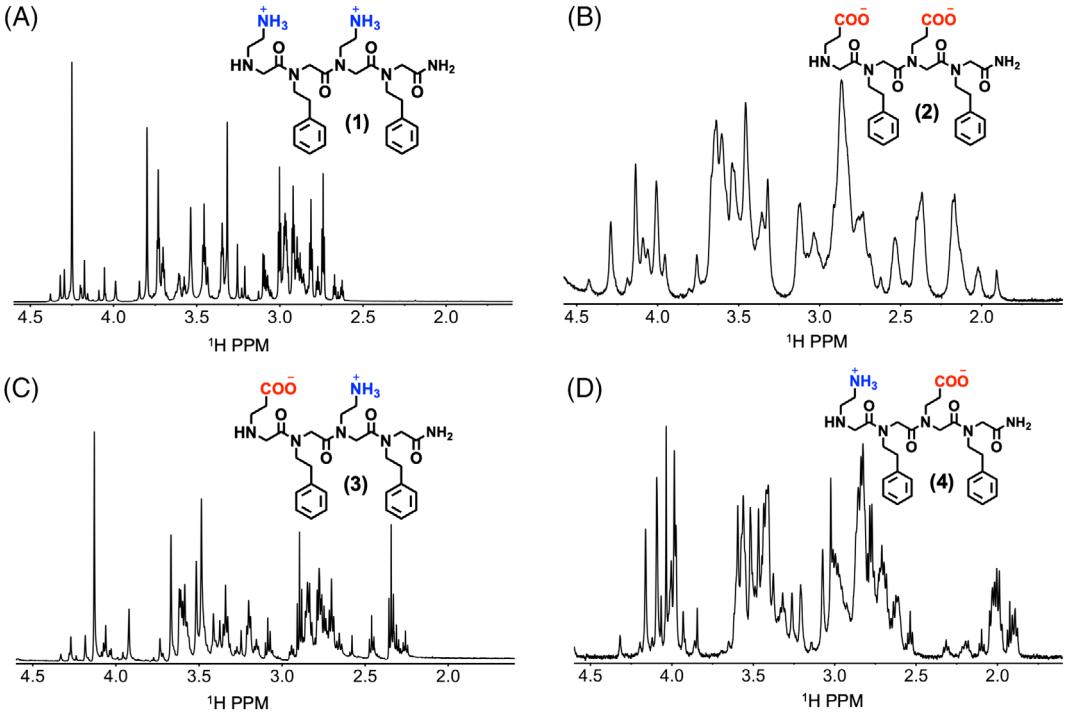

FIGURE 2 1D ^{1}H NMR spectra of the four peptoids in 90% D_2O and 10% sodium phosphate buffer at pH 7.4 in water (A) peptoid **1**, (B) peptoid **2**, (C) peptoid **3**, (D) peptoid **4**

contrast level (Supporting Information Figure S7 and Figure S13), indicating greater than two major conformers. Peptoid **3** similarly displayed 12 intense correlations (Supporting Information Figure S9), indicating one predominant conformation. HSQC conformational homogeneity analyses were consistent with 1D ^{1}H data (Figure 2).

All 12 peptoid **1** ^{1}H-^{13}C pairs were identified at a high contour view of the ^{1}H-^{13}C HSQC spectrum. Each correlation arises from a ^{1}H directly bonded to a ^{13}C, allowing us to take advantage of ^{13}C shift values in successive assignment experiments. Correlations are grouped according to their position on the peptoid chain, with distinct clusters for BB, SC1 and SC2 type peaks. The cluster types have strong grouping along the ^{13}C axis, with R2 BB being a noteworthy outlier in the BB type. As would be expected, the clustering is weaker in the ^{1}H axis, but separates SC2 protons from those closer to the BB.

3.4 | COSY

We established connectivity of the two sidechain methylene groups within a single residue via 2D COSY.[20] As can be seen in Figure 5, four strong cross peaks associated with the sidechains of the major conformation were clearly visible in the spectrum, allowing for identification of the four pairs of sidechain CH_2 resonances. Transferring the proton

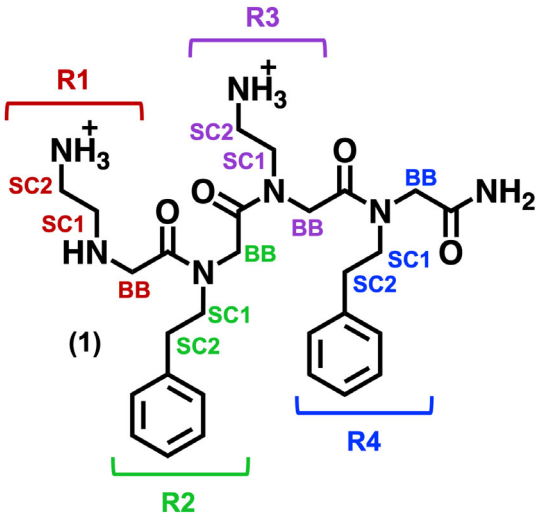

FIGURE 3 Atom labeling scheme for peptoid **1**. The four residues (R) each have their own backbone methylene (BB) and two sidechain methylenes (SC1 and SC2). The sequence is Nae-Npe-Nae-Npe

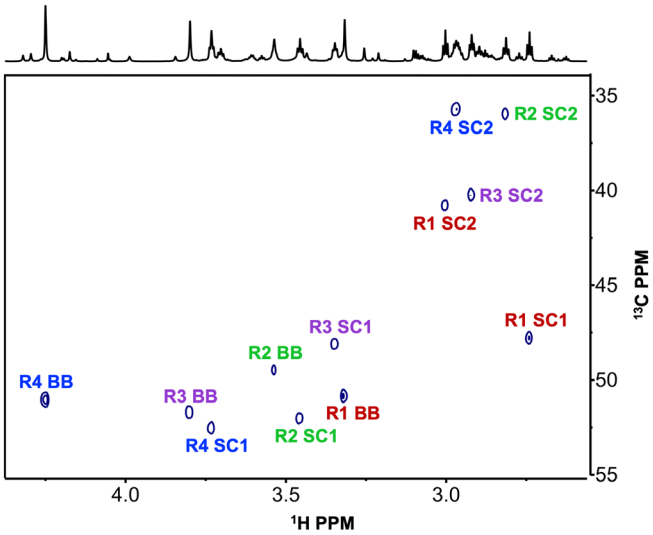

FIGURE 4 ^{1}H-^{13}C HSQC spectrum of peptoid **1** at a high contour threshold, showing both backbone and sidechain correlations for all four residues of the major conformer

10970282, 2019, 6, Downloaded from https://onlinelibrary.wiley.com/doi/10.1002/bip.23267 by University Of California, Wiley Online Library on [10/02/2026]. See the Terms and Conditions (https://onlinelibrary.wiley.com/terms-and-conditions) on Wiley Online Library for rules of use; OA articles are governed by the applicable Creative Commons License

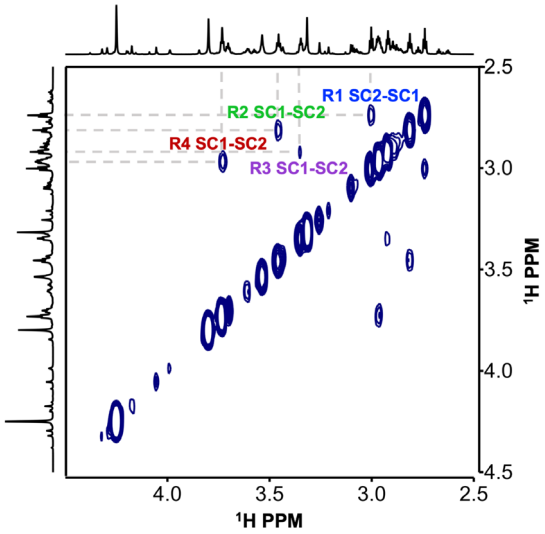

FIGURE 5 2D COSY spectrum of peptoid **1** showing correlations between sidechain atoms SC1 and SC2 for each residue in the major conformer

shifts to the HSQC spectrum, the corresponding ^{1}H-^{13}C signals were catalogued as belonging to sidechains, and the ^{13}C signals for each of the side chain's ethyl groups was determined. The four remaining peaks in the HSQC spectrum were classified as belonging to backbone CH_2 groups. Because the backbone CH_2 groups are isolated, that is, have no proton neighbors, they do not appear in the COSY spectrum, allowing us to analyze each sidechain independently.

3.5 | HMBC

Each sidechain SC1 CH_2 resonance correlated with its own backbone alpha carbon resonance via three-bond proton-carbon couplings in an HMBC experiment[14] (Figure 6). Additionally, the SC2 proton resonances of the two aromatic groups were identified through correlations between the SC2 CH_2 protons and carbon resonances of its own aromatic group (Supporting Information Figure S4), providing classification of the spin systems as belonging to Nae or Npe residues. ^{1}H-^{13}C HMBC experiments have been used previously to sequentially assign adjacent backbone CH_2 groups to one another in peptoids using correlations between carbonyl carbons.[21] In the case of peptoid **1**, overlap of ^{13}CO resonances made sequential assignment by this method difficult. We therefore developed a new method based on 1,*n*-Adequate experiments.

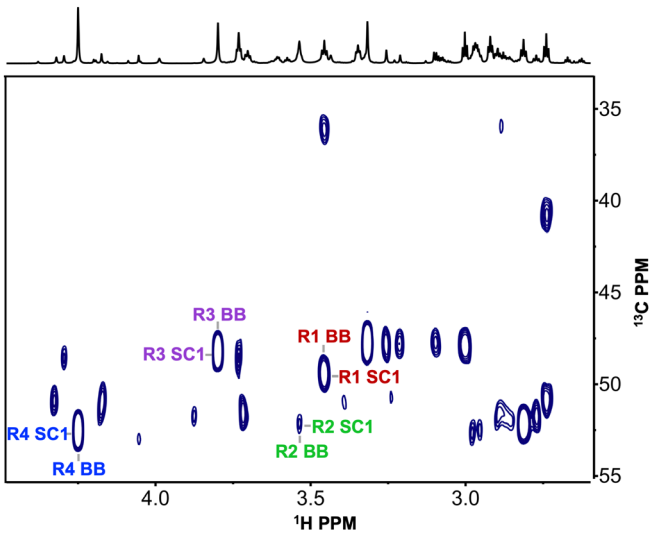

FIGURE 6 2D ^{1}H-^{13}C HMBC spectrum of peptoid **1**. Correlations between backbone protons and the sidechain carbon atoms of SC1 for the major form are labeled. These correlations were used to connect the sidechain and backbone resonances

3.6 | 1,*n*-Adequate

Because the HMBC data did not allow us to assign the sequential backbone methylene group connectivity, we developed a new sequential assignment method based on 1,*n*-Adequate experiments.[22] In the protein ubiquitin, three-bond Ca-Ca coupling constants range from one to two Hertz.[23] We reasoned that the three-bond coupling constants in our peptoids should have similar values, and could be useful for making sequential assignments. The Adequate family of experiments is often used in the assignment of the ^{1}H and ^{13}C resonances of small molecules.[24] Of interest here was the 1,*n*-Adequate experiment which correlates protons with carbons several bonds removed via multi-bond carbon-carbon couplings. It is typically employed on samples without ^{13}C enrichment. In our case, to increase sensitivity, all the backbone alpha carbons of peptoid **1** were specifically labeled with ^{13}C to make peptoid **5** (Table 1). This was readily achieved by using bromoacetic acid-2-^{13}C during routine submonomer synthesis.[14,15]

A 1,*n*-Adequate spectrum of peptoid **5** is shown in Figure 7. Weak one-bond ^{1}H-^{13}C correlations for each of the backbone resonances appear opposite in phase (blue) to the stronger cross peaks (green). Strong cross peaks can be seen, which correlate each backbone proton with the ^{13}C resonances of neighboring residues. For example, backbone proton R3 at 3.80 ppm (R3 BB) is correlated to carbon

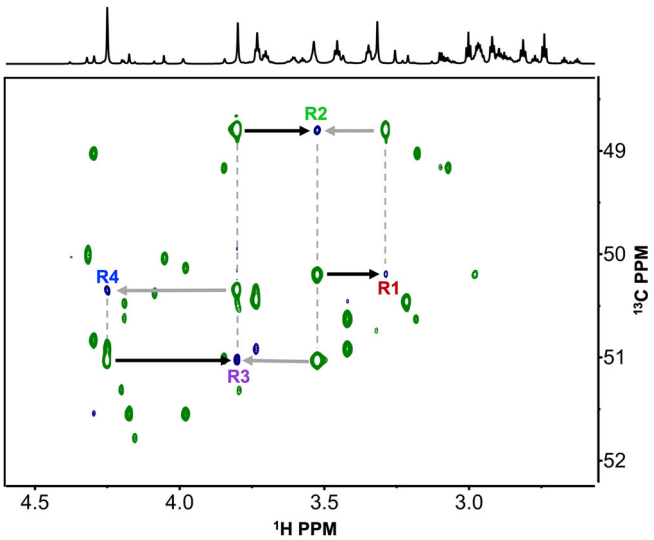

FIGURE 7 1,*n*-Adequate spectrum of peptoid **5** labeled with ^{13}C at all backbone positions. Blue peaks correspond to one-bond ^{1}H-^{13}C correlations, and are labeled with residue number for the major form. The green peaks result from magnetization transfer to adjacent ^{13}C spins (dashed lines), allowing for sequential assignment of the peptoid backbone (black/gray arrows)

10970282, 2019, 6, Downloaded from https://onlinelibrary.wiley.com/doi/10.1002/bip.23267 by University Of California, Wiley Online Library on [10/02/2026]. See the Terms and Conditions (https://onlinelibrary.wiley.com/terms-and-conditions) on Wiley Online Library for rules of use; OA articles are governed by the applicable Creative Commons License

atoms at 48.8 ppm and 50.4 ppm, corresponding to the carbon resonances of R2 and R4, respectively. These data were sufficient to determine the connections between backbone ^{1}H-^{13}C signals for the major conformer. Together with residue type assignments from the HMBC experiment, we were able to unambiguously assign the chain directionality and all backbone and sidechain ethyl resonances for this conformer.

3.7 | ROESY

ROESY experiments[25] use the Nuclear Overhauser effect to give pairs of protons with separations of less than 5 Å. ROESY experiments can be used to identify peptoid backbone *cis/trans* patterns using ROEs that arise between backbone alpha carbon protons to identify *cis* amide bonds, and a lack of ROEs between backbone protons to infer *trans* amide bonds.[7] Upon analysis of the ROESY spectra for the major conform of peptoid **1** (Figure 8A), an ROE was observed between the backbone protons of R2 and R3, indicating a backbone pattern of *trans-cis-trans*. An additional inter-residue ROE was observed between R1 backbone (BB) and R2 sidechain 1 (SC1). Both observed distance constraints can be rationalized in minimized molecular dynamics model (Figure 8C) as described below. Other ROEs arise from expected intra-residue correlations.

3.8 | Minor conformation structural analysis

In order to determine the *cis-trans* backbone pattern of the minor conformers, we employed 3D NMR techniques because of their low abundance and spectral crowding. Based on the success of the 1,*n*-Adequate experiment in correlating neighboring ^{13}C spins along the peptoid backbone, we hypothesized that 3D hCCH-TOCSY and HcCH-TOCSY experiments[26] could be used to assign the backbone ^{1}H and ^{13}C resonances of the minor forms, in analogy to the use of these experiments in assignment of protein sidechain resonances. The advantage of the HCCH-TOCSY methods over the 2D 1,*n*-Adequate is that it is possible to correlate all four ^{1}H and ^{13}C resonances of a conformer with each ^{1}H-^{13}C pair, rather than just the ^{13}C resonances of neighboring residues. Another advantage is that the data are separated into three dimensions, helping to resolve this crowded region of the spectrum.

hCCH-TOCSY (Supporting Information Figure S17) and HcCH-TOCSY (Supporting Information Figure S18) spectra were used to catalog four ^{1}H-^{13}C correlations for five conformers and three ^{1}H-^{13}C correlations for one conformer. An HcCH-TOCSY experiment with a shorter mixing time (Supporting Information Figure S19) was then used to identify neighbors in analogy to the COSY experiment, and hence, the relative order of the resonances. Even though the order of the resonances was now known, the start and end of each sequence remained ambiguous. The ambiguity was resolved by identifying the ^{1}H-^{13}C pairs for all of the R1 residues from an HSQC spectrum recorded on a sample in which only the R1 position was labeled with ^{13}C (peptoid **6**). To confirm the assignments, the ^{1}H-^{13}C resonances of residues R2, R3, and R4 were also identified from HSQC spectra of singly labeled samples (peptoids **7**-**9**). Integrated peaks of these singly labeled samples were also used to determine the abundance of each conformer (Supporting Information Table S1).

The *cis-trans* configuration of the three predominate forms were determined from ROEs observed in a 2D ^{1}H-^{13}C HSQC-ROESY spectrum (Supporting Information Figure S16). The 2D ^{1}H-^{13}C version was chosen to alleviate signal overlap of ^{1}H signals in the 2D ^{1}H-^{1}H ROESY. For further confirmation, additional HSQC-ROESY spectra (Supporting Information Figure S21, S23, S25, and S27) were recorded on each of the singly labeled peptoids (peptoids **6**-**9**). Interestingly, the three highest abundance conformers, which in total represent 80% of ensemble population, exhibit a *cis* amide bond between R2 and R3 (Table 2).

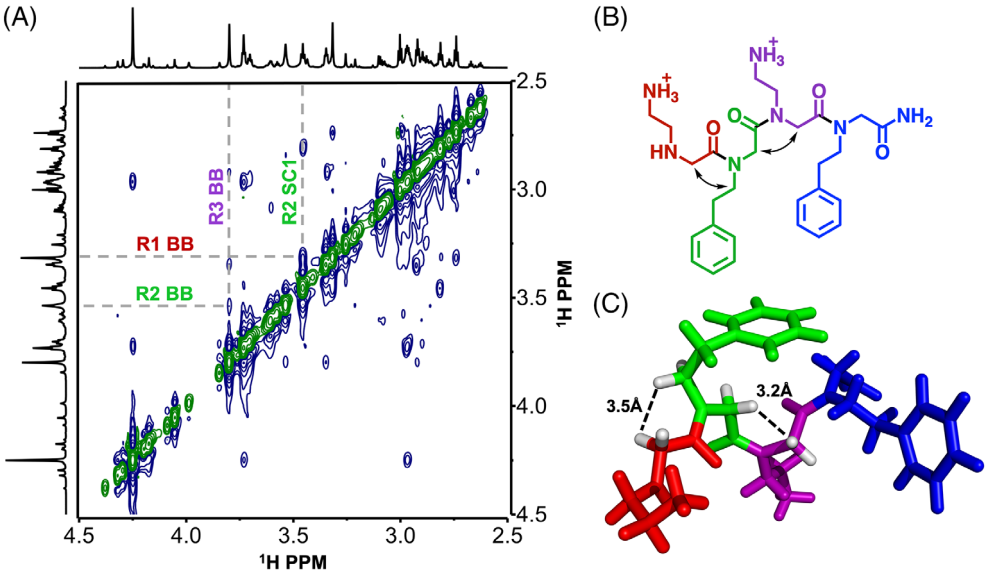

FIGURE 8 (A) 2D ROESY spectrum of peptoid **1**. Blue peaks correspond to ROEs, indicating that the protons are close in space (<5 Å). (B) For the major conformer, ROEs are observed between backbone (BB) protons of R2 and R3, and between the backbone (BB) protons of R1 and the SC1 sidechain protons of R2. (C) Inter-proton distances, superimposed on a molecular dynamics minimized structure, are indicated by dashed lines. Distances are reported as the average between the four protons in each ROE correlation

10970282, 2019, 6, Downloaded from https://onlinelibrary.wiley.com/doi/10.1002/bip.23267 by University Of California, Wiley Online Library on [10/02/2026]. See the Terms and Conditions (https://onlinelibrary.wiley.com/terms-and-conditions) on Wiley Online Library for rules of use; OA articles are governed by the applicable Creative Commons License

TABLE 2 Predominant conformations of peptoid 1

Conformer	Abundance (%)	Backbone *cis/trans* pattern
1 (major)	52	*trans-cis-trans*
2	18	*cis-cis-trans*
3	10	*trans-cis-cis*

3.9 | Major conformation of peptoid 3

As was the case for peptoid **1**, the 1D ^{1}H and 2D HSQC spectra indicated the presence of a major conformation. A similar conformation analysis was applied to the major conformation of peptoid **3**. Results showed similar inter-residue ROEs between R2 BB and R3 BB, indicative of a *cis* amide bond, and between R1 BB and R2 SC1. The sequence identity of the two central residues in peptoids **1** and **3**, Npe-Nae, suggest that these play an important role in stabilization of the major conformation. Molecular dynamics modeling and quantum mechanics computations were done to help elucidate stabilizing interactions.

3.10 | Molecular dynamics simulation

Classical molecular dynamics simulations were performed on peptoid **1** in water. We simulated the predominant (as determined by NMR) *trans-cis-trans* backbone pattern of this compound (conformer 1, Table 2). Simulations were run using the NAMD package for 10 ns, the last 5 ns of which were analyzed for conformational preferences.

The simulations indicate that the 3-dimensional backbone trace is well preserved over the trajectory, while there is significant variation in side chain orientations (Figure 9A). In all cases, the structures were consistent with the distance constraints derived from the ROESY experiment (Figure 8C). Further analysis of the backbone dihedral angles for the central two residues, R2 and R3, was performed because they are internal and separated from the chain termini. Over the last 5 ns of simulation time, we computed the dihedral angles on a Ramachandran plot (Figure 9B). Interestingly, the spread in dihedral angles was very narrow for both of these residues, and they populate the known energy minima of the Ac-Sar-Sar-N(Me)$_2$ Ramachandran plot.[27] Specifically, residue 2 and residue 3 occupy the Z_{Rt} and Z_{Sc} conformations, respectively.[28]

3.11 | Quantum mechanics modeling

We asked whether the observed preference for the *cis* conformation at the central amide bond might be driven by backbone interactions with the Nae side chain. We first surveyed the relative conformational energies of a simple peptoid monomer model compound: protonated *N*-(2-aminoethyl)-*N*-methylacetamide (Supporting Information Figure S28). The lowest energy conformation (by ~5 kcal/mol) contained a *cis* amide bond with a hydrogen bond between the ammonium group and the carbonyl (Supporting Information Table S2).

For more detailed predictions of the types of internal interactions that may stabilize the solution structure, we analyzed a series of peptoid **1** geometries via DFT. We used two levels of theory B3LYP/6-311G** and M06-2X/6-311G**, both in implicit water solvent (see methods for further details). The overall lowest energy structure predicted by B3LYP features hydrogen bonds between the central Nae amine and both the preceding and succeeding carbonyl oxygens (Figure 10A). The second most favorable B3LYP structure (Figure 10B, 0.98 kcal/mol relative energy) is similar but the central *Nae* only participates in a single hydrogen bond (with its neighboring *N*-terminal carbonyl). Also in this structure, the *N*-terminal Nae amino and *C*-terminal amide are both involved in hydrogen bonds with their nearest backbone carbonyls. The lowest energy M06-2X structure (Figure 10C) is a compact reverse turn, reminiscent of a touch-turn.[29,30]The central Nae hydrogen bonds with its neighboring *N*-terminal carbonyl and the *N*-terminal Nae participates in both a hydrogen bond with the *C*-terminal carbonyl and a π-cation interaction with the second Npe side chain. The second lowest energy M06-2X geometry (Figure 10D, 0.46 kcal/mol relative energy) features the central Nae forming a hydrogen bond with both of the following backbone carbonyls rather than with its neighboring *N*-terminal carbonyl. The *N*-terminal Nae side chain also participates in a hydrogen bond with the *C*-terminal carbonyl and a π-cation interaction with the fourth Npe. The more compact geometries of the tetramer optimized by

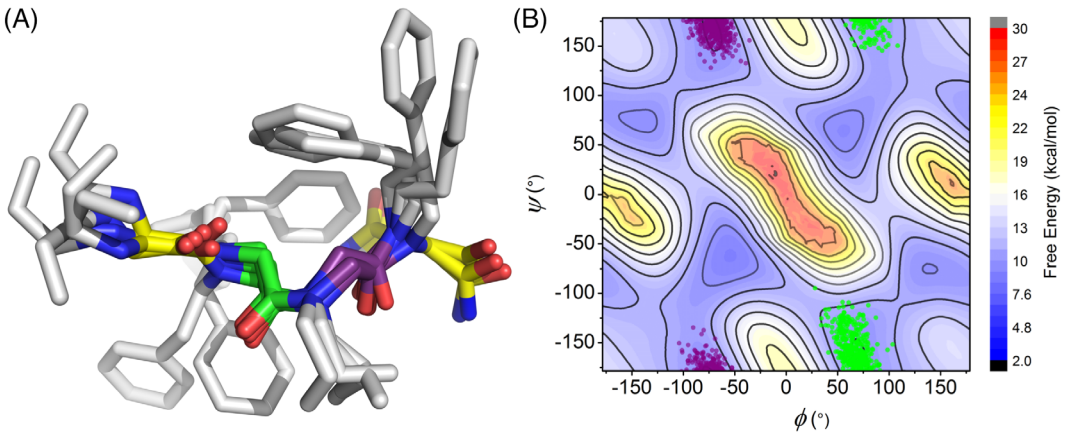

FIGURE 9 Molecular dynamics simulation of compound **1**, confined to a *trans-cis-trans* backbone configuration, as determined by NMR, reveals a predominant backbone conformation. (A) Overlay of five structural snapshots from the last 5 ns of the molecular dynamics simulation trajectory. (B) The two internal peptoid monomers, residue 2 (green), and residue 3 (purple) have well-defined dihedral angles as overlaid on a *cis* Ramachandran plot[27] that fall within known energy minima for peptoids

10970282, 2019, 6, Downloaded from https://onlinelibrary.wiley.com/doi/10.1002/bip.23267 by University Of California, Wiley Online Library on [10/02/2026]. See the Terms and Conditions (https://onlinelibrary.wiley.com/terms-and-conditions) on Wiley Online Library for rules of use; OA articles are governed by the applicable Creative Commons License

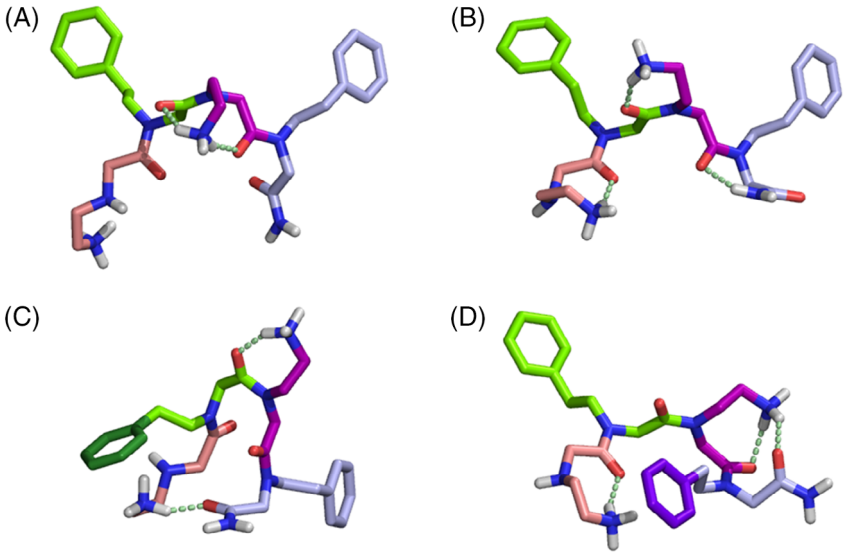

FIGURE 10 The two lowest energy sampled geometries of peptoid **1** as predicted by B3LYP/6-311G** (A) and (B); and by M06-2X/6-311G** (C) and (D). Both DFT models included PCM solvent water. Hydrogen bonds are highlighted in light green and Npe aromatic carbons involved in π-cation interactions are shaded darker

M06-2X are likely due to the better representation of dispersion forces in this functional driving self-interaction.

4 | CONCLUSIONS

We use a simple model peptoid to demonstrate a new, straightforward and broadly applicable peptoid backbone resonance assignment method. The procedure uses the 1,*n*-Adequate experiment with selective ^{13}C labeling of backbone alpha carbons to correlate protons of each backbone to the carbon of a neighboring residue backbone alpha carbon, thus efficiently assigning backbone connectivity. This method is ideally suited for the study of peptoids, as backbone labeling is readily achieved using commercially available bromoacetic acid-2-^{13}C as a submonomer. This method addresses an inherent challenge faced in peptoid NMR, as the absence of the backbone nitrogen protons precludes the use of many NMR tools available for peptides. While we demonstrate this method on tetramers, it is expected to be applicable to longer peptoid chains because of this new ability to correlate any given monomer to its direct neighbors. Additionally, we successfully apply 3D HCCH-TOCSY spectra on peptoids labeled with ^{13}C at all backbone alpha carbons.

We find that a peptoid tetramer with unconstrained sidechains has a predominant conformation (>50%) in aqueous solution. Furthermore, >80% of the total conformers contain a *cis* amide bond at the central amide bond (between R2 and R3). The degree of conformational homogeneity was considerably higher than expected. Dihedral angles taken from molecular dynamics simulations of the *trans-cis-trans* configuration fall into narrow regions which coincide with the expected low energy wells of the peptoid Ramachandran plot. The clear impact of these low energy wells on peptoid conformation will be essential for the predictive design of folded peptoids.

NMR analysis of peptoid **1** and peptoid **3**, as well as quantum mechanical calculations, suggest that the central residues (Npe-Nae) play an important role in stabilizing conformation. Most low energy structures obtained from quantum mechanical calculations suggest the presence of a hydrogen bond between the central Nae residue and its neighboring *N*-terminal carbonyl. It is likely that this structural motif, which is repeated seven times in succession in the nanosheet forming sequence Block 28, plays a role in the assembly of highly ordered supramolecular structures. The Nae residue itself may be useful for future conformational control of peptoid chains without requiring the use of sterically congested or large hydrophobic sidechains. Most importantly, this deeper understanding of the intrinsic conformational preferences of minimally constrained peptoid oligomers should facilitate the rational design of folded peptoids.

ACKNOWLEDGMENTS

Work at the Molecular Foundry was supported by the Office of Science, Office of Basic Energy Sciences, of the U.S. Department of Energy under Contract No. DE-AC02-05CH11231 and the DARPA-fold F(x) program. Funds for the 900 MHz NMR spectrometer were provided by the NIH through grant GM68933 to D.W. QM calculations were carried out on the High-Performance Computing resources at New York University Abu Dhabi. The authors declare no conflict of interest.

ORCID

Ronald N. Zuckermann https://orcid.org/0000-0002-3055-8860

REFERENCES

[1] A. M. Rosales, H. K. Murnen, S. R. Kline, R. N. Zuckermann, R. A. Segalman, *Soft Matter* **2012**, *8*, 3673.
[2] Y. Gao, T. Kodadek, *Chem. Biol.* **2013**, *20*, 360.
[3] S. B. Y. Shin, B. Yoo, L. J. Todaro, K. Kirshenbaum, *J. Am. Chem. Soc.* **2007**, *129*, 3218.
[4] Q. Sui, D. Borchardt, D. L. Rabenstein, *J. Am. Chem. Soc.* **2007**, *129*, 12042.

10970282, 2019, 6, Downloaded from https://onlinelibrary.wiley.com/doi/10.1002/bip.23267 by University Of California, Wiley Online Library on [10/02/2026]. See the Terms and Conditions (https://onlinelibrary.wiley.com/terms-and-conditions) on Wiley Online Library for rules of use; OA articles are governed by the applicable Creative Commons License

[5] B. C. Gorske, E. M. Mumford, C. G. Gerrity, I. Ko, *J. Am. Chem. Soc.* **2017**, *139*, 8070.
[6] J. R. Stringer, J. A. Crapster, I. A. Guzei, H. E. Blackwell, *J. Am. Chem. Soc.* **2011**, *133*, 15559.
[7] K. Huang, C. W. Wu, T. J. Sanborn, J. A. Patch, K. Kirshenbaum, R. N. Zuckermann, A. E. Barron, I. Radhakrishnan, *J. Am. Chem. Soc.* **2006**, *128*, 1733.
[8] B. C. Gorske, R. C. Nelson, Z. S. Bowden, T. A. Kufe, A. M. Childs, *J. Org. Chem.* **2013**, *78*, 11172.
[9] C. Caumes, O. Roy, S. Faure, C. Taillefumier, *J. Am. Chem. Soc.* **2012**, *134*, 9553.
[10] A. S. Knight, E. Y. Zhou, M. B. Francis, R. N. Zuckermann, *Adv. Mater.* **2015**, *27*, 5665.
[11] E. J. Robertson, A. Battigelli, C. Proulx, R. V. Mannige, T. K. Haxton, L. Yun, S. Whitelam, R. N. Zuckermann, *Acc. Chem. Res.* **2016**, *49*, 379.
[12] B. C. Hudson, A. Battigelli, M. D. Connolly, J. Edison, R. K. Spencer, S. Whitelam, R. N. Zuckermann, A. K. Paravastu, *J. Phys. Chem. Lett.* **2018**, *9*, 2574.
[13] D. Marion, *Mol. Cell. Proteomics: MCP* **2013**, *12*, 3006.
[14] E. K. Bradley, J. M. Kerr, L. S. Richter, G. M. Figliozzi, D. A. Goff, R. N. Zuckermann, D. C. Spellmeyer, J. M. Blaney, *Mol. Divers.* **1997**, *3*, 1.
[15] R. N. Zuckermann, J. M. Kerr, S. B. H. Kent, W. H. Moos, *J. Am. Chem. Soc.* **1992**, *114*, 10646.
[16] J. C. Phillips, R. Braun, W. Wang, J. Gumbart, E. Tajkhorshid, E. Villa, C. Chipot, R. D. Skeel, L. Kale, K. Schulten, *J. Comput. Chem.* **2005**, *26*, 1781.
[17] D. T. Mirijanian, R. V. Mannige, R. N. Zuckermann, S. Whitelam, *J. Comput. Chem.* **2014**, *35*, 360.
[18] Frisch, M. J.; Trucks, G. W.; Schlegel, H. B.; Scuseria, G. E.; Robb, M. A.; Cheeseman, J. R.; Scalmani, G.; Barone, V.; Petersson, G. A.; Nakatsuji, H.; Li, X.; Caricato, M.; Marenich, A. V.; Bloino, J.; Janesko, B. G.; Gomperts, R.; Mennucci, B.; Hratchian, H. P.; Ortiz, J. V.; Izmaylov, A. F.; Sonnenberg, J. L.; Williams; Ding, F.; Lipparini, F.; Egidi, F.; Goings, J.; Peng, B.; Petrone, A.; Henderson, T.; Ranasinghe, D.; Zakrzewski, V. G.; Gao, J.; Rega, N.; Zheng, G.; Liang, W.; Hada, M.; Ehara, M.; Toyota, K.; Fukuda, R.; Hasegawa, J.; Ishida, M.; Nakajima, T.; Honda, Y.; Kitao, O.; Nakai, H.; Vreven, T.; Throssell, K.; Montgomery Jr., J. A.; Peralta, J. E.; Ogliaro, F.; Bearpark, M. J.; Heyd, J. J.; Brothers, E. N.; Kudin, K. N.; Staroverov, V. N.; Keith, T. A.; Kobayashi, R.; Normand, J.; Raghavachari, K.; Rendell, A. P.; Burant, J. C.; Iyengar, S. S.; Tomasi, J.; Cossi, M.; Millam, J. M.; Klene, M.; Adamo, C.; Cammi, R.; Ochterski, J. W.; Martin, R. L.; Morokuma, K.; Farkas, O.; Foresman, J. B.; Fox, D. J., Gaussian, Inc. Wallingford, CT, **2016**.
[19] J. A. Crapster, J. R. Stringer, I. A. Guzei, H. E. Blackwell, *Biopolymers* **2011**, *96*, 604.
[20] W. F. Reynolds, R. G. Enríquez, *J. Nat. Prod.* **2002**, *65*, 221.
[21] P. Armand, K. Kirshenbaum, R. A. Goldsmith, S. Farr-Jones, A. E. Barron, K. T. V. Truong, K. A. Dill, D. F. Mierke, F. E. Cohen, R. N. Zuckermann, E. K. Bradley, *Proc. Natl. Acad. Sci.* **1998**, *95*, 4309.
[22] M. Reibarkh, R. T. Williamson, G. E. Martin, W. Bermel, *J. Magn. Reson.* **2013**, *236*, 126.
[23] M. Hennig, W. Bermel, H. Schwalbe, C. Griesinger, *J. Am. Chem. Soc.* **2000**, *122*, 6268.
[24] G. E. Martin, in *Annual Reports on NMR Spectroscopy* (Ed: G. A. Webb), Academic Press, Cambridge, MA, **2011**, p. 215.
[25] T. L. Hwang, A. J. Shaka, *J. Am. Chem. Soc.* **1992**, *114*, 3157.
[26] L. E. Kay, G. Y. Xu, A. U. Singer, D. R. Muhandiram, J. D. Forman-Kay, *J. Magn. Reson. Ser. B* **1993**, *101*, 333.
[27] J. R. Edison, R. K. Spencer, G. L. Butterfoss, B. C. Hudson, A. I. Hochbaum, A. K. Paravastu, R. N. Zuckermann, S. Whitelam, *Proc. Natl. Acad. Sci.* **2018**, *115*, 5647.
[28] R. K. Spencer, G. L. Butterfoss, J. R. Edison, J. Eastwood, S. Whitelam, K. Kirshenbaum, R. N. Zuckermann, *Biopolymers* **2019**, e23266.
[29] G. L. Butterfoss, K. Drew, P. D. Renfrew, K. Kirshenbaum, R. Bonneau, *Biopolymers* **2014**, *102*, 369.
[30] L. L. Videau, W. B. Arendall, J. S. Richardson, *Proteins: Struct. Funct. Bioinform.* **2004**, *56*, 298.

SUPPORTING INFORMATION

Additional supporting information may be found online in the Supporting Information section at the end of this article.

How to cite this article: Roe LT, Pelton JG, Edison JR, et al. Unconstrained peptoid tetramer exhibits a predominant conformation in aqueous solution. *Biopolymers*. 2019;110:e23267. https://doi.org/10.1002/bip.23267

10970282, 2019, 6, Downloaded from https://onlinelibrary.wiley.com/doi/10.1002/bip.23267 by University Of California, Wiley Online Library on [10/02/2026]. See the Terms and Conditions (https://onlinelibrary.wiley.com/terms-and-conditions) on Wiley Online Library for rules of use; OA articles are governed by the applicable Creative Commons License